J Biol Phys (2014) 40:313–323
DOI 10.1007/s10867-014-9350-3

ORIGINAL PAPER

Probing the coordination properties of glutathione with transition metal ions (Cr^{2+}, Mn^{2+}, Fe^{2+}, Co^{2+}, Ni^{2+}, Cu^{2+}, Zn^{2+}, Cd^{2+}, Hg^{2+}) by density functional theory

Jianhua Liu · Hongxia Liu · Yan Li · Haijun Wang

Received: 14 November 2013 / Accepted: 14 April 2014 / Published online: 14 June 2014

Abstract Complexes formed by reduced glutathione (GSH) with metal cations (Cr^{2+}, Mn^{2+}, Fe^{2+}, Co^{2+}, Ni^{2+}, Cu^{2+}, Zn^{2+}, Cd^{2+}, Hg^{2+}) were systematically investigated by the density functional theory (DFT). The results showed that the interactions of the metal cations with GSH resulted in nine different stable complexes and many factors had an effect on the binding energy. Generally, for the same period of metal ions, the binding energies ranked in the order of $Cu^{2+} > Ni^{2+} > Co^{2+} > Fe^{2+} > Cr^{2+} > Zn^{2+} > Mn^{2+}$; and for the same group of metal ions, the general trend of binding energies was $Zn^{2+} > Hg^{2+} > Cd^{2+}$. Moreover, the amounts of charge transferred from S or N to transition metal cations are greater than that of O atoms. For Fe^{2+}, Co^{2+}, Ni^{2+}, Cu^{2+}, Zn^{2+}, Cd^{2+} and Hg^{2+} complexes, the values of the Wiberg bond indices (WBIs) of M-S (M denotes metal cations) were larger than that of M-N and M-O; for Cr^{2+} complexes, most of the WBIs of M-O in complexes were higher than that of M-S and M-N. Furthermore, the changes in the electron configuration of the metal cations before and after chelate reaction revealed that Cu^{2+}, Ni^{2+}, Co^{2+} and Hg^{2+} had obvious tendencies to be reduced to Cu^{+}, Ni^{+}, Co^{+} and Hg^{+} during the coordination process.

Keywords Glutathione · Metal complex · Density functional theory NBO analysis

Electronic supplementary material The online version of this article (doi:10.1007/s10867-014-9350-3) contains supplementary material, which is available to authorized users.

J. Liu · H. Liu · Y. Li · H. Wang (✉)
School of Chemical and Material Engineering, Jiangnan University, Wuxi, Jiangsu, 214122, People's Republic of China
e-mail: wanghj329@outlook.com

J. Liu
Yibin University Computational Physics Key Laboratory of Sichuan province, School of Chemistry and Chemical Engineering, Yibin University, Yibin, Sichuan 644000, People's Republic of China

1 Introduction

Reduced glutathione (GSH) is a ubiquitous thiol-containing tripeptide (γ - glutamyl - cysteinyl - glycine). GSH has many cellular functions, including detoxication of xenobiotics and heavy metals, reduction of oxidation-prone protein thiols, maintenance of cellular membranes and deactivation of free radicals [1]. The intracellular concentrations of reduced glutathione vary from 1 to 20 mM and alternations in the level of cellular GSH have been related to a number of diseases, such as diabetes, human immunodeficiency virus infection, cystic fibrous, acute respiratory distress syndrome and chronic renal failure [2]. Due to its intracellular abundance, GSH is a likely target for metal cations, especially those having high affinity for thiolate sulfur [3]. It has been suggested that GSH may serve as a primary defense against metal cation toxicity [4, 5]. Reduced glutathione (GSH), present in nuclei at concentrations ranging from 1 and 10 mM, has been implied as a protective agent against heavy metal cation toxicity through forming complexes [6–11].

Copper is essential for many processes in bioorganisms. However, excess copper can result in marked reactive oxygen species (ROS) formation that can damage lipids, nucleic acids and proteins [12, 13]. Increased free or redox active copper can also lead to the degradation of extracellular GSH, by which it exerts its harmful effects [14]. Although zinc is essential for cellular function, sustained increases in free Zn^{2+} levels are harmful. A cell-death mechanism and mitochondrial dysfunction are initiated though a Zn^{2+}-induced loss of cellular antioxidant capacity by depleting cellular reduced glutathione [15]. Intracellular nickel is responsible for neoplastic transformation and excess Ni (II) is a human carcinogen [12]. The intracellular level of reduced GSH is an important factor in the process of cellular resistance to Ni (II) [16]. Cobalt is essential to humans as it is a necessary component of vitamin B12 [17]. However, higher concentrations of cobalt display carcinogenic properties and induce the generation of ROS [18]. Manganese is also involved in the initial formation of ROS and their subsequent reactions with macromolecules such as proteins, lipids, polysaccharides and nucleic acids leading to altered membrane fluidity, loss of enzyme activity and genomic damage [19]. The toxicologic characteristics of mercury (elemental, inorganic and organic forms) and its ability to react with and deplete free sulfhydryl groups are well-known [20]. It is demonstrated that the administration of mercury as Hg (II) to rats results in increased hydrogen peroxide formation, glutathione depletion and lipid peroxidation in kidney mitochondria [21].

Knowledge of the coordination chemistry of GSH is essential to understand the defense mechanism of GSH against metal cation toxicity. Moreover, GSH, possessing all kinds of biological donor atoms (two carboxyls, one thiol, one amino and two pairs of carbonyls and amide donors within two peptide bonds) is a versatile ligand, forming stable complexes with both hard and soft metal cations [22, 23]. Thus, the coordination chemistry of glutathione is also important as it serves as a model system for binding metal cations of larger peptide and protein molecules [24, 25].

Different experimental techniques have been devoted to investigate the metal complexes of GSH, such as electron paramagnetic resonance (EPR) [26, 27], NMR [28, 29], X-ray diffraction (X-ray) [30, 31] and ESI-MS [32]. Nevertheless, it is difficult to explain the structures of the complexes at the atomic and electronic level. Computational studies can fill this gap and provide thermochemical, kinetic and structural information [33]. Furthermore, the different affinities of a specific ligand for different metal cations, which play a key role in the function and properties of metal-containing biomolecules, can also be obtained directly by quantum-chemical computations [34, 35].

The coordination details of complexes formed by Cd^{2+} with GSH and 3-mercaptopropionic acid were explored using the quantum-chemical computation method [36, 37]. In order to explore the metal-binding selectivity and specificity of GSH from the perspective of structure and energy properties, we investigated the coordination behavior of transition metal cations (Cr^{2+}, Mn^{2+}, Fe^{2+}, Co^{2+}, Ni^{2+}, Cu^{2+}, Zn^{2+}, Cd^{2+}, Hg^{2+}) with GSH in a gas phase using the density functional method. The density functional method (DFT) is reliable and one of the most popular tools to describe metal-ligand interactions in biological systems, due to its excellent performance-to-cost ratio. Structural and electronic characterizations of the complexes formed by metal ions with amino acids were studied by the DFT method [38, 39].The interaction between metal ions and organic molecules in the gas phase is an ideal environment from which complexation mechanisms can be obtained in the absence of any complicating solvent effects.

2 Computational methods

Calculations for structure optimization were performed at the DFT level using the Becke's three parameter hybrid exchange functional and the gradient-corrected non-local functional of Lee et al. (B3LYP) [40, 42]. The 6-31G (d, p) basis set was used for describing H, C, O, N and S atoms, whereas the LANL2DZ pseudopotential [43] was adopted for metal cations. The stability of the optimized geometries was verified by performing calculations on vibrational frequencies. Natural bond orbital (NBO) analysis [44] was applied to analyze the charge transfer, natural population analysis and Wiberg bond indices of the complexes. All computations reported in this work were carried out using the Gaussian 03 program [45].

Open shell calculations (Cr^{2+}, Mn^{2+}, Fe^{2+}, Co^{2+}, Ni^{2+}, Cu^{2+}) were carried out using spin-unrestricted formalism. The stable spin states for Cr^{2+}, Mn^{2+} and Cu^{2+} are quintet, sextet and doublet, respectively. A more complicated case is with Fe^{2+}, Co^{2+} and Ni^{2+} ions, which may exist in their complexes both in high-spin and low-spin states. The geometries with various spin configurations are optimized and the lowest energy structures are chosen for further analysis. Thus, the more stable quintet state for Fe^{2+}, quartet state for Co^{2+}, triplet state for Ni^{2+} ion are considered. Zn^{2+}, Cd^{2+} and Hg^{2+} are d^{10} cations; their complexes are a closed-shell system with singlet ground state.

The binding energies (ΔE) of A (GSH) monomers with B (metal cation) are calculated as the energy difference between the complexes and respective donor-acceptor moieties. For systems under consideration, it is defined as:

$$\Delta E = E_{AB} - (E_A + E_B)\,. \tag{1}$$

Here, E_{AB} is the energy of the complexes; $E_{A,}$ the energy of GSH; E_B, the energy of metal cations. The binding energies are corrected by zero-point energy (ZPE) and basis set superposition errors (BSSE) with the counterpoise procedure method proposed by Boys and Bernardi [46] and van Duijneveldt et al. [47].

3 Results and discussion

The reduced GSH molecule is flexible, and different stable conformations of the ligand may coexist in solution and in the gas phase. The folded form in the gas phase is more stable than

the extended form, while in aqueous solutions the extended form is more stable because of hydrogen bonds between the water molecules and GSH [41]. A recent B3LYP quantum-mechanical investigation found that hydrogen bonding interactions between the terminal ends of glutathione resulted in a "basket-like" conformation and this basket–conformation was one of the most stable structures in the gas phase [48].

The aim of our work goes beyond the conformational aspects of GSH. Thus, here, the stable structure ("basket-like" conformation) of GSH is considered [48] (shown in Fig. 1) and only the GSH: M^+ stoichiometric ratio of 1:1 has been taken into account.

3.1 Coordination mode

All possible modes of complexation are calculated and the complexes are examined by selecting systematically. Nine stable complexes are gained and the complexes (mono-, di-, tri- , tetra- and penta-coordinating) labeled as GSH-M-1a, GSH-M-1b, GSH-M-2a, GSH-M-2b, GSH-M-3a, GSH-M-3b, GSH-M-4 and GSH-M-5 (M=Cr^{2+}, Mn^{2+}, Fe^{2+}, Co^{2+}, Ni^{2+}, Cu^{2+}, Zn^{2+}, Cd^{2+}, Hg^{2+}) are summarized in Fig. 2.

In the complex GSH-M-1a, the metal cations are monocoordinated to glutathione with complexation to the sulfur (S29) atom of the Cys residue. In the presence of Cr^{2+}, Mn^{2+}, Fe^{2+}, Co^{2+}, $Ni^{2+}$and Cu^{2+}, the intramolecular hydrogen bond of the terminal end (O36-H37···O7) in free GSH is broken after optimization. Furthermore, the terminal carboxyl of glutamyl residue of GSH has the tendency to be detached in the GSH-M-1a complexes (M=Cr^{2+}, Mn^{2+}, Ni^{2+}, Cu^{2+}). The bond length of C4-C6 of GSH (1.61∼1.64 Å) in those complexes is lengthened comparing to the bond length in the free GSH (1.51 Å). Moreover, the Fe^{2+}, Co^{2+}, Zn^{2+}, Cd^{2+} and Hg^{2+} ions promote hydrogen transfer from the S atom of

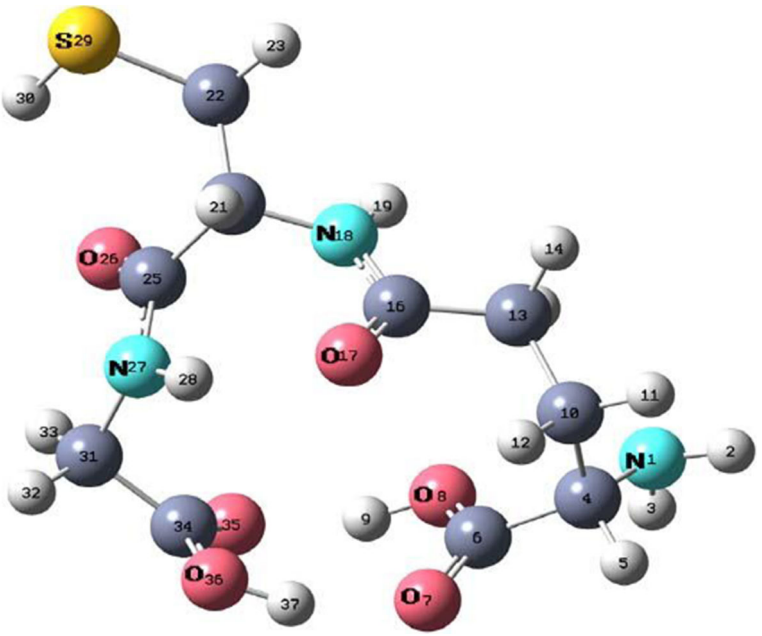

Fig. 1 The glutathione conformation. Color codes: O, red; N, blue; S, yellow; C, deep grey; H, light grey

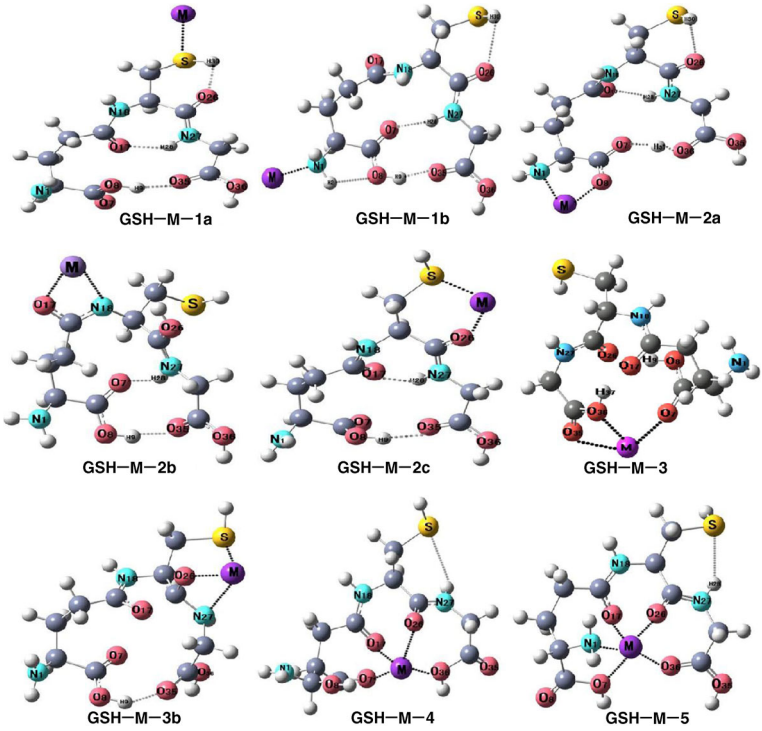

Fig. 2 The optimized electronic structures of the metal complexes (GSH-M, M= Cr^{2+}, Mn^{2+}, Fe^{2+}, Co^{2+}, Ni^{2+}, Cu^{2+}, Zn^{2+}, Cd^{2+}, Hg^{2+}) calculated by B3LYP

thiol to the O26 atom in the carbonyl of the Cys residue. The metal cations are monocoordinated to the amine group (N1) of glutamyl residue in the complexes GSH-M-1-b. The intramolecular hydrogen bonds of the terminal end (O36-H37$\cdots$O7 and N27-H28$\cdots$O17) in free GSH are broken and form two new intramolecular hydrogen bonds (N27-H28$\cdots$O7 and N1-H2$\cdots$O8) in GSH-M-1b.

In complexes 2a, 2b and 2c, the metal cations appear to be bicoordinated. In complexes 2a, an oxygen atom arising from the carboxylic of the Gly residue (O8) and a nitrogen atom from the amine group of the glutamyl of the residue (N1) are involved in the coordination. The intramolecular hydrogen bond of the terminal end (O8-H9...O35) in free GSH is destroyed and the H9 transfers from O8 to O35. Metal cations are bicoordinated to O17 and N18 of Glu residue in GSH-M-2b, to the sulfur (S29) and oxygen (O26) of the carbonyl of the Cys residue in GSH-M-2c. The intramolecular hydrogen bond of the terminal end (O36-H37$\cdots$O7) in free GSH is broken and new intramolecular hydrogen (N27-H28$\cdots$O7) in GSH-M-2b is formed.

The GSH-M-3a and GSH-M-3b complexes have tridentated complexation to O7, O35, O36 and O26, N27, S29 of GSH, respectively. For Cr^{2+} and Zn^{2+} complexes, the carbon (C25) atom and O (17) atom of carbonyl are inclined to be a covalent bond (five-membered ring configuration is formed within C16, O17, C25, C20 and N18) in GSH-M-3b.

In the GSH-M-4a complexes, the atoms directly involved in the interaction with metal cations belong to the carboxylic group of Glu and Gly residue (O7, O36), to the carbonyl of the peptide bond of Glu (O17) and to the oxygen atom of the carbonyl of the Cys residue (O26).

Metal ions are pentacoordinated with GSH in GSH-M-5. The ligand atoms involved in the coordination include two oxygen atoms from the carboxylic group (O35, O8), two oxygen atoms from both carbonyls (O17, O26) and a nitrogen atom of the amine group (N1).

We also tried to identify more metal cation coordination sites for GSH. But, after optimization, no further structures beyond the GSH-M complexes described above were obtained.

3.2 Energies analysis

The values of the binding energies indicated the binding capacity of the metal cation with GSH and the deformation energy (E_{def}) of GSH was used to estimate the deformation of GSH during the formation of the complex from an energy point of view. Deformation energy was measured by the single-point energy differences between the free fragment and the corresponding isolated moiety in the complex (the remaining part of the metal ion was set as the ghost atom).

The binding energies and their absolute values are shown in Table S1 (Supplementary information) and Fig. 3, respectively. The negative values of the binding energies indicate that all the complexes are stable and that the stability of the complex improves with the increase of the absolute value of the binding energy.

For the same period for metal ions, the absolute values of the binding energies of the metal ions with GSH in complexes decrease from Cr^{2+} to Mn^{2+}, increase monotonically again from Mn^{2+} to Cu^{2+} and then decrease sharply from Cu^{2+} to Zn^{2+}. Generally, the binding energies ranked in the order of $Cu^{2+} > Ni^{2+} > Co^{2+} > Fe^{2+} > Cr^{2+} > Zn^{2+} > Mn^{2+}$. For the same group of metal ions, the general trend of binding energies was $Zn^{2+} > Hg^{2+} > Cd^{2+}$. From Cr^{2+} to Ni^{2+}, the trend of the binding energies is consistent with that of the ion potential (z/r) of the metal cations as shown in Table 1. The value of the ion potential is equal to the ratio of electric charge and the radius of the metal ion. The high ion potential of the metal cation results in large binding energy between metal cations and GSH. However, there are some exceptions: the ion potential of Ni^{2+} (2.90) is larger than that of

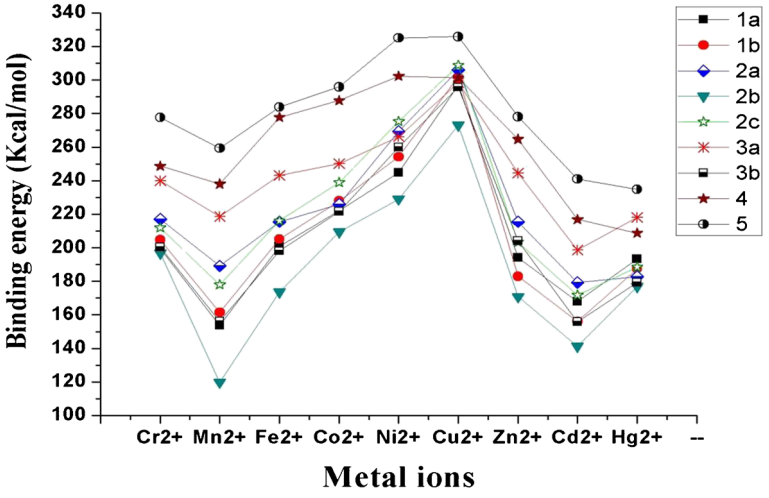

Fig. 3 The absolute values of binding energies of metal ions with GSH in complex calculated by B3LYP (M= Cr^{2+}, Mn^{2+}, Fe^{2+}, Co^{2+}, Ni^{2+}, Cu^{2+}, Zn^{2+}, Cd^{2+}, Hg^{2+})

Table 1 The radii for metal ions (r in Å, coordination number is 6, from Lange's Handbook of Chemistry) and the ion potential (z/r) of alkali and alkaline earth metal cations

	Cr^{2+}	Mn^{2+}	Fe^{2+}	Co^{2+}	Ni^{2+}	Cu^{2+}	Zn^{2+}	Cd^{2+}	Hg^{2+}
Z	2	2	2	2	2	2	2	2	2
R	0.80	0.83	0.78	0.745	0.69	0.73	0.74	0.95	1.02
I	2.50	2.41	2.56	2.68	2.90	2.74	2.70	2.11	1.96

Cu^{2+} (2.74), while the absolute values of binding energies of Ni^{2+} are smaller than or equal to that of Cu^{2+}. This might be due to the different ground-state electronic configurations ($3d^8$ for Ni^{2+}, $3d^9$ for Cu^{2+}). Cu^{2+} is more inclined to obtain electrons from the ligand to be a fully occupied 3d orbital ($3d^{10}$) than is Ni^{2+}, which enhances the interactions between the metal ion and ligand atom. Moreover, the differences of the ion potential of Cu^{2+} (2.74) and Zn^{2+} (2.70) are not obvious, while the binding energies of Zn^{2+} with GSH in complexes are significantly smaller than that of Cu^{2+}. All of the d orbitals of the Zn^{2+} are occupied and the interaction between Zn 3d and the heteroatom (O, N and S) orbitals becomes very small. The same group of metal ions Zn^{2+}, Cd^{2+} and Hg^{2+} are d^{10} ions and the order of the ion potential is $Zn^{2+} > Cd^{2+} > Hg^{2+}$. Due to the small electron screening of 4f of Hg^{2+} to outer electrons and the small difference in radii between Cd^{2+} and Hg^{2+}, the effective nuclear charge of Hg^{2+} is larger than that of Cd^{2+}. Thus, the binding energies of Hg^{2+} with GSH in some complexes are larger than that of Cd^{2+}.

In general, the binding energies are proportional to the coordination number, although there are some exceptions. The binding energies of GSH-M-2b are the smallest for all metal ions; the differences of the binding energy of Cu^{2+} and GSH in GSH-M-1, GSH-M-2 and GSH-M-3, as well as GSH-M-4 are very tiny; for Ni^{2+}, the binding energy of GSH-M-3a is smaller than that of GSH-M-2a and GSH-M-2c; for Hg^{2+}, the binding energy of GSH-M-3a is larger than that of GSH-M-4. This may due to several factors, such as: the deformation energy of GSH during coordination to the metal cations, electrostatic interaction, metal-ligand repulsion and charge transfer [49]. Moreover, the above-mentioned factors might behave variously for different metal cations and different coordination modes.

In order to better combine with metal cations, GSH is required to deform from equilibrium geometry to the geometrical conformation in the complex. As shown in Table 2, the

Table 2 The deformation energies ΔE_{def} (kcal/mol) of the GSH in complexes calculated by B3LYP (M= Cr^{2+}, Mn^{2+}, Fe^{2+}, Co^{2+}, Ni^{2+}, Cu^{2+}, Zn^{2+}, Cd^{2+}, Hg^{2+})

	Cr^{2+}	Mn^{2+}	Fe^{2+}	Co^{2+}	Ni^{2+}	Cu^{2+}	Zn^{2+}	Cd^{2+}	Hg^{2+}
GSH-M-1a	22.3	18.23	36.31	40.14	22.84	23.0	44.40	41.8	42.0
GSH-M-1b	33.9	34.49	34.31	33.99	34.06	34.1	16.51	14.0	31.4
GSH-M-2a	62.9	59.55	34.75	28.36	44.09	43.6	54.82	45.6	28.1
GSH-M-2b	86.5	82.13	34.38	83.77	48.91	42.7	40.69	32.9	74.9
GSH-M-2c	17.8	17.97	18.85	26.13	27.72	27.1	17.03	14.4	13.9
GSH-M-3a	81.7	75.74	78.59	80.99	82.72	35.0	17.78	71.7	81.0
GSH-M-3b	88.2	19.67	21.08	24.39	25.98	25.5	77.89	12.2	11.1
GSH-M-4	48.2	46.56	50.29	50.71	50.15	38.9	47.19	44.7	43.3
GSH-M-5	55.7	50.68	52.31	53.96	54.09	53.3	51.42	45.9	43.2

positive value of Edef illustrates that the geometry distortion during the formation of GSH is an energy rising process. So, Edef is a repulsive contribution during the coordination process. Moreover, with different metal cations and coordination modes, the deformation degree of GSH varies. Furthermore, the binding and deformation energies are not lineally correlated.

3.3 NBO population analysis

Natural bond orbital (NBO) analysis, which helps to understand the details during the coordination process, is adopted to calculate the charge transfer (CT), Wiberg bond indices (WBIs) and the natural electron configuration (NEC) of the metal ions in the complexes. The charge transfer (the charge decrement values on corresponding metal ions in complexes going from isolated ions to metal-complexes) between metal cations and GSH in complexes is listed in Table 3. The results show that the charge transfer takes place in all complexes during the complexation reaction, which implies the presence of an interaction with a covalent contribution. The overlaps in metal-ligand bonds almost occurs between a hybrid sd orbital of metal ions (Cr^{2+}, Mn^{2+}, Fe^{2+}, Co^{2+}, Ni^{2+}, Cu^{2+}, Zn^{2+}, Cd^{2+}, Hg^{2+}) and a 2p orbital of oxygen and nitrogen, 3p orbital of sulfur. Cu^{2+} has more charge transfer character than the other metal cations in the complexes, while Zn^{2+} and Cd^{2+} undergo the relative minimal charge transfer. This can be related to the different ground-state electronic configurations ($3d^9$ for Cu^{2+}, $3d^{10}$ and $4d^{10}$ for Zn^{2+} and Cd^{2+}, respectively), Cu^{2+} has the greatest tendency to be a fully occupied $3d^{10}$ orbital. Due to a large effective nuclear charge, the charge transfer between Hg^{2+} and GSH is more than that of Zn^{2+} and Cd^{2+}.

It was also found that the amounts of charge transferred from S or N to metal ions are greater than that from O atoms to metal ions. For example, the amounts of charge transfer in monodentate GSH-M-1a and GSH-M-1b are much more than that in GSH-M-4 and GSH-M-5. This charge transfer suggests that a higher degree of covalent bond may be involved between the S or N and metal ions than that of between O and metal ions. Furthermore, the larger amount of charge transfer also indicates the stronger bonding of transition metal ions with the S and N.

The natural electron configurations calculated for metal cations in these complexes are shown in Table S2. The electron transfer is mainly into 4s and 3d and only a little into the 4p orbital of metal ions (Cr^{2+}, Mn^{2+}, Fe^{2+}, Co^{2+}, Ni^{2+}, Cu^{2+}) and the electrons from the

Table 3 The charge transfer between metal ions and GSH in complexes (M= Cr^{2+}, Mn^{2+}, Fe^{2+}, Co^{2+}, Ni^{2+}, Cu^{2+}, Zn^{2+}, Cd^{2+}, Hg^{2+})

	Cr^{2+}	Mn^{2+}	Fe^{2+}	Co^{2+}	Ni^{2+}	Cu^{2+}	Zn^{2+}	Cd^{2+}	Hg^{2+}
GSH-M-1a	1.15	1.06	1.04	1.07	1.21	1.22	0.87	0.88	1.11
GSH-M-1b	1.27	1.13	1.16	1.16	1.17	1.17	1.09	1.08	1.34
GSH-M-2a	0.56	0.77	0.84	1.19	1.24	1.21	0.60	0.49	0.91
GSH-M-2b	0.65	0.53	0.94	0.73	1.20	1.16	0.58	0.70	0.94
GSH-M-2c	1.04	0.71	1.14	1.26	1.31	1.26	0.66	0.75	1.01
GSH-M-3a	0.67	0.52	0.60	0.67	0.74	1.24	0.41	0.46	0.70
GSH-M-3b	0.74	0.85	1.06	1.27	1.26	1.30	0.44	0.87	1.18
GSH-M-4	0.72	0.63	0.71	0.76	0.79	1.08	0.27	0.41	0.49
GSH-M-5	0.92	0.69	0.80	0.86	0.91	0.95	0.29	0.47	0.54

ligand enter mainly to the 4s and a little to the 4p orbital for Zn^{2+}, Cd^{2+} and Hg^{2+}. The naked Cu^{2+} ion has a natural electron configuration of 3d9 and the natural electron configuration changes to $4s^{(0.19\sim0.29)}3d^{(9.33\sim9.94)}4p^{(0.01\sim0.35)}$ in the complexes. It was found that the electron configuration of Cu^{2+} in most of the complexes is very close to Cu^{+} ($3d^{10}$), which reveals that Cu^{2+} in these complexes has been reduced to Cu^{+} during the coordination with GSH. Moreover, the reduction tendencies also occur with other metal cations in some complexes, especially in the monodentate complexes (GSH-M-1 and GSH-M-2), in which the amounts of charge transfer from GSH to metal cations are more than that of other complexes. The same reduction tendencies also occurred with the Ni^{2+}, Co^{2+} and Hg^{2+} complexes.

The Wiberg bond index (WBI), bond orders and the bond distances of the metal-ligand are summarized in Table S3. For the same metal ion, the trend of the bond length follows M-S > M-N > M-O, while the trends of M –S, M-N and M-O from Cr^{2+} to Hg^{2+} are irregular. For example, the radius of Ni^{2+} is shorter than that of Cu^{2+} (0.69 vs. 0.73 Å), while the distance between Ni-S is longer than that of Cu-S (2.27 Å and 2.25 Å in GSH-M-1a, respectively). Thus, the bond distance of the metal-ligand is related to the atom radii of the metal and ligand, as well as to the coordination site and the binding strength of the metal-ligand. The values of the WBI indicate significant bonding interactions between the metal ions and the coordination atoms (O, S, N), as well as the presence of a covalent contribution. The WBIs for the same metal-ligand bond are various in different complexes. Generally, the WBIs of M-S are larger than that of M-N and M-O for complexes of Fe^{2+}, Co^{2+}, Ni^{2+}, Cu^{2+}, Zn^{2+}, Cd^{2+} and Hg^{2+}; the differences of the WBI of M-O, M-S and M-N for Mn^{2+} are not significant; for Cr^{2+} complexes, most of the WBIs of M-O in complexes are higher than those of M-S and M-N and the difference of M-S and M-N is not obvious.

4 Conclusions

In this work, the interaction between metal ions with GSH was systematically explored at both the electronic and molecular levels in the gas phase. The ion potential, the electron configuration and the coordination numbers of the metal ions, as well as the chelate site and type of heteroatom of GSH played important roles in determining the coordination properties of metal cations and GSH. The results obtained here could provide valuable insight into the coordination preferences, binding strengths and binding geometries of GSH complexes and add a useful piece of knowledge to the field of interactions of transition metal cations with biological molecules. As the solvent effect might cause some changes in the structure and thermochemical properties, much work remains to be done. Further deeper examinations need to be carried out to investigate the interaction of metal cations with GSH in solution using a PCM model.

Acknowledgments The authors are grateful to the Project Fund of the Sichuan Education Department (12ZB350) and the Doctoral Candidate Foundation of Jiangnan University (JUDCF11033) for financial support.

References

1. Sies, H.: Glutathione and its role in cellular functions. Free Rad. Biol. Med. **27**, 916–921 (1999)
2. Krężel, A., Bal, W.: Studies of zinc (II) and nickel (II) complexes of GSH, GSSG and their analogs shed more light on their biological relevance. Bioinorg. Chem. Appl. **2**, 293–305 (2004)

3. Hinchman, C.A., Ballatori, N.: Glutathione conjugation and conversion to mercapturic acids can occur as an intrahepatic process. J. Toxicol. Environ. Health **41**, 387–409 (1994)
4. Rauser, W.E.: Phytochelatins and related peptides. Structure, biosynthesis, and function. Plant Physiol. **109**, 1141–1149 (1995)
5. Wang, K., Lu, J., Li, R.: The events that occur when cisplatin encounters cells. Coordin. Chem. Rev. **151**, 53–88 (1996)
6. Lynn, S., Yew, F.H., Hwang, J.W., et al.: Glutathione can rescue the inhibitory effects of nickel on DNA ligation and repair synthesis. Carcinog. **15**, 2811–2816 (1994)
7. Formicka-Kozlowska, G., Kozlowska, H.: Coordination ability of thyrotropin releasing factor. II. Nickel (II) complexes with TRF. Inorg. Chim. Acta. **46**, 29–34 (1980)
8. Li, W., Zhao, Y., Cou, I.N.: Alterations in cytoskeletal protein sulfhydryls and cellular glutathione in cultured cells exposed to cadmium and nickel ions. Toxicol. **77**, 65–79 (1993)
9. Bal, W., Kozłowski, H., Kasprzak, K.S.: Molecular models in nickel carcinogenesis. J. Inorg. Biochem. **79**, 213–218 (2000)
10. Speisky, H., Gómez, M., Burgos-Bravo, F., et al.: Generation of superoxide radicals by copper–glutathione complexes: redox-consequences associated with their interaction with reduced glutathione. Bioorg. Med. Chem. **17**, 1803–1810 (2009)
11. Salnikow, K., Gao, M., Voitkun, V., et al.: Altered oxidative stress responses in nickel-resistant mammalian cells. Cancer Res. **54**, 6407–6412 (1994)
12. Bal, W., Kasprzak, K.S.: Induction of oxidative DNA damage by carcinogenic metals. Toxicol. Lett. **127**, 55–62 (2002)
13. Kim, B.E., Nevitt, T., Thiele, D.J.: Mechanisms for copper acquisition, distribution and regulations. Nat. Chem. Biol. **4**, 176–185 (2008)
14. Pope, S.A.S., Milton, R., Heales, S.J.R.: Astrocytes protect against copper-catalysed loss of extracellular glutathione. Neurochem. Res. **33**, 1410–1418 (2008)
15. Wiseman, D.A., Sharma, S., Black, S.M.: Elevated zinc induces endothelial apoptosis via disruption of glutathione metabolism: role of the ADP translocator. Biometals. **23**, 19–30 (2010)
16. Li, W., Zhao, Y., Chou, I.N.: Mg^{2+}antagonism on Ni^{2+}-induced changes in microtubule assembly and cellular thiol homeostasis. Toxicol. Appl. Pharmacol. **136**, 101–111 (1996)
17. Galanis, A., Karapetsas, A., Sandaltzopoulos, R.: Metal-induced carcinogenesis, oxidative stress and hypoxia signalling. Mut. Res. **674**, 31–35 (2009)
18. Valko, M., Morris, H., Cronin, M.: Metals toxicity and oxidative stress. Curr. Med. Chem. **12**, 1161–1208 (2005)
19. Shi, Q., Bao, Z., He, Y., et al.: Silicon-mediated alleviation of Mn toxicity in Cucumis sativus in relation to activities of superoxide dismutase and ascorbate peroxidase. Phytochemistry **66**, 1551–1559 (2005)
20. Goyer, R.A.: Toxic effects of metals. In: Amdur, M.O., Doull, J., Klaassen, C.D. (eds.) Casarett and Doull's Toxicology: the Basic Science of Poisons. 4th edn., pp. 629–681. Pergamon Press, New York (1991)
21. Lund, B.O., Miller, D.M., Woods, J.S.: Studies on Hg (II)-induced H_2O_2 formation and oxidative stress in vivo and in vitro in rat kidney mitochondria. Biochem. Pharmacol. **45**, 2017–2024 (1993)
22. Krężel, A., Bal, W.: Coordination chemistry of glutathione. Acta. Biochim. Pol. **46**, 567–580 (1999)
23. Krężel, A., Wójcik, J., Bal, W.: May GSH and L-His contribute to intracellular binding of zinc? Thermodynamic and solution structural study of a ternary complex. Chem. Commun. **6**, 704–705 (2003)
24. Kilyén, M., Forg, P., Lakatos, A., et al.: Interaction of Al(III) with the peptides AspAsp and AspAspAsp. J. Inorg. Biochem. **94**, 207–213 (2003)
25. Helbig, K., Bleuel, C., Krauss, G.J., et al.: Glutathione and transition-metal homeostasis in Escherichia coli. J. Bacteriol. **190**, 5431–5438 (2008)
26. Dimitrova, M., Turmanova, S., Vassilev, K.: Complexes of glutathione with heavy metals as catalysts for oxidation. Reac. Kinet. Mech. Cat. **99**, 69–78 (2010)
27. Mukherjea, K.K., Panda, G.: Selim, M.: Biophysical, spectroscopic and biochemical investigation of DNA-Cu(II)-GSH interactions, Transition. Met. Chem. **33**, 203–210 (2008)
28. Delalande, O., Desvaux, H., Godat, E., et al.: Cadmium-glutathione solution structures provide new insights into heavy metal detoxification. FEBS J. **277**, 5086–5096 (2010)
29. Martinez-Finley, E.J., Aschner, M.: Revelations from the nematode caenorhabditis elegans on the complex interplay of metal toxicological mechanisms. J. Toxicol. **2011**, 895–236 (2011)
30. Wang, X., Li, K., Yang, X.D., et al.: Complexation of Al (III) with reduced glutathione in acidic aqueous solutions. J. Inorg. Biochem. **103**, 657–665 (2009)
31. Zhang, J., Li, J., Zhang, J., Xie, R.: Aqueous synthesis of ZnSe nanocrystals by using glutathione as ligand: the pH-mediated coordination of Zn^{2+} with glutathione. J. Phys. Chem. C **114**, 11087–11091 (2010)

32. Połeć-Pawlak, K., Ruzik, R., Lipiec, E.: Investigation of Cd(II), Pb(II) and Cu(I) complexation by glutathione and its component amino acids by ESI-MS and size exclusion chromatography coupled to ICP-MS and ESI-MS. Talanta **72**, 1564–1572 (2007)
33. Belcastro, M., Marino, T., Russo, N., et al.: Interaction of cysteine with Cu^{2+} and group IIb (Zn^{2+}, Cd^{2+}, Hg^{2+}) metal cations: a theoretical study. J. Mass. Spectrom. **40**, 300–306 (2005)
34. Marino, T., Russo, N., Toscano, M.: Gas-phase metal ion (Li^{+}, Na^{+}, Cu^{+}) affinities of glycine and alanine. J. Inorg. Biochem. **79**, 179–185 (2000)
35. Mineva, T., Neshev, N., Russo, N., et al.: Density functional computations and mass spectrometric measurements. Can this coupling enlarge the knowledge of gas-phase chemistry? Adv. Quantum Chem. **36**, 93–120 (1999)
36. Belcastro, M., Marino, T., Russo, N., et al.: Structure and coordination modes in the interaction between Cd^{2+} and 3-mercaptopropionic acid. J. Phys. Chem. A **108**, 8407–8410 (2004)
37. Belcastro, M., Marino, T., Russo, N., et al.: The role of glutathione in cadmium ion detoxification: Corrdination modes and binding properties- a density functional study. J. Inorg. Biochem. **103**, 50–57 (2009)
38. Pushie, M.J., Rauk, A., Jirik, F.R., et al.: Can copper binding to the prion protein generate a misfolded form of the protein? Biometals **22**, 159–175 (2009)
39. Marino, T., Toscano, M., Russo, N., et al.: Structural and electronic characterization of the complexes obtained by the interaction between bare and hydrated first-row transition-metal ions (Mn^{2+}, Fe^{2+}, Co^{2+}, Ni^{2+}, Cu^{2+}, Zn^{2+}) and glycine. J. Phys. Chem. B **110**, 24666–24673 (2006)
40. Becke, A.D.: Density-functional exchange-energy approximation with correct asymptotic behavior. Phys. Rev. A: At. Mol. Opt. Phys. **38**, 3098–3100 (1988)
41. Becke, A.D.: Density-functional thermochemistry. III. The role of exact exchange. J. Chem. Phys. **98**, 5648–5652 (1993)
42. Lee, C., Yang, W., Parr, R.G.: Development of the Colle-Salvetti correlation-energy formula into a functional of the electron density. Phys. Rev. B: Condens. Matter. **37**, 785–789 (1988)
43. Hay, P.J., Wadt, W.R.: Ab initio effective core potentials for molecular calculations. Potentials for K to Au including the outermost core orbitals. J. Chem. Phys. **82**, 270–276 (1985)
44. Reed, A.E., Curtiss, L.A., Weinhold, F.: Intermolecular interactions from a natural bond orbital, donor-acceptor viewpoint. Chem. Rev. **88**, 899–926 (1988)
45. Frisch, M.J., Trucks, G.W., Schlegel, H.B., Scuseria, G.E., Robb, M.A., Cheeseman, J.R., Montgomery, J.A. Jr., Vreven, T., Kudin, K.N., Burant, J.C., Millam, J.M., Iyengar, S.S., Tomasi, J., Barone, V., Mennucci, B., Cossi, M., Scalmani, G., Rega, N., Petersson, G.A., Nakatsuji, H., Hada, M., Ehara, M., Toyota, K., Fukuda, R., Hasegawa, J., Ishida, M., Nakajima, T., Honda, Y., Kitao, O., Nakai, H., Klene, M., Li, X., Knox, J.E., Hratchian, H.P., Cross, J.B., Bakken, V., Adamo, C., Jaramillo, J., Gomperts, R., Stratmann, R.E., Yazyev, O., Austin, A.J., Cammi, R., Pomelli, C., Ochterski, J.W., Ayala, P.Y., Morokuma, K., Voth, G.A., Salvador, P., Dannenberg, J.J., Zakrzewski, V.G., Dapprich, S., Daniels, A.D., Strain, M.C., Farkas, O., Malick, D.K., Rabuck, A.D., Raghavachari, K., Foresman, J.B., Ortiz, J.V., Cui, Q., Baboul, A.G., Clifford, S., Cioslowski, J., Stefanov, B.B., Liu, G., Liashenko, A., Piskorz, P., Komaromi, I., Martin, R.L., Fox, D.J., Keith, T., Al-Laham, M.A., Peng, C.Y., Nanayakkara, A., Challacombe, M., Gill, P.M.W., Johnson, B., Chen, W., Wong, M.W., Gonzalez, C., Pople, J.A.: Gaussian 03, revision A.1; Gaussian, Inc., Wallingford, CT (2004)
46. Boys, S., Bernardi, F.: The calculation of small molecular interactions by the differences of separate total energies. Some procedures with reduced errors. Mol. Phys. **19**, 553–566 (1970)
47. van Duijneveldt, F.B., van Duijneveldt-van de Rijdt, J.G.C.M., van Lenthe, J.H.: State of the art in counterpoise theory. Chem. Rev. **94**, 1873–1885 (1994)
48. Ding, V.Z.Y., Dawson, S.S.H., Lau, L.W.Y., et al.: A computational study of glutathione and its fragments: n-acetylcisteinylglycine and γ-glutamylmethylamide. Chem. Phys. Lett. **507**, 168–173 (2011)
49. Bertrán, J., Rodríguez-Santiago, L., Sodupe, M.: The different nature of bonding in Cu^{+}-Glycine and Cu^{2+}-Glycine. J. Phys. Chem. B **103**, 2310–2317 (1999)